Geophysical Journal International

Geophys. J. Int. (2020) **222,** 1952–1964
Advance Access publication 2020 June 04
Marine Geosciences and Applied Geophysics

doi: 10.1093/gji/ggaa277

Field surveys and numerical modelling of the 2004 December 26 Indian Ocean tsunami in the area of Mumbai, west coast of India

Mohammad Heidarzadeh [1], Alexander Rabinovich,[2,3] Satoshi Kusumoto[4] and C.P. Rajendran[5]

[1] *Department of Civil and Environmental Engineering, Brunel University London, Uxbridge UB83PH, UK. E-mail: mohammad.heidarzadeh@brunel.ac.uk*
[2] *Institute of Ocean Sciences, Sidney, BC V8L 4B2, Canada*
[3] *Shirshov Institute of Oceanology, Russian Academy of Sciences, Moscow* 117997, *Russia*
[4] *Japan Agency for Marine-Earth Science and Technology, Yokohama* 236-0001, *Japan*
[5] *Jawaharlal Nehru Centre for Advanced Scientific Research, Bangalore* 560064, *India*

Accepted 2020 May 29. Received 2020 May 13; in original form 2019 January 27

ABSTRACT

In the aftermath of the 2004 Indian Ocean (Sumatra-Andaman) tsunami, numerous survey teams investigated its effects on various locations across the Indian Ocean. However, these efforts were focused only on sites that experienced major destruction and a high death toll. As a consequence, some Indian Ocean coastal megacities were not examined. Among the cities not surveyed was Mumbai, the principal west coast port and economical capital of India with a population of more than 12 million. Mumbai is at risk of tsunamis from two major subduction zones in the Indian Ocean: the Sumatra–Andaman subduction zone (SASZ) and the Makran subduction zone (MSZ). As a part of the present study, we conducted a field survey of the 2004 Indian Ocean tsunami effects in Mumbai, analysed the available tide gauge records and performed tsunami simulations. Our field survey in 2018 January found run-up heights of 1.6−3.3 m in the Mumbai area. According to our analysis of tide gauge data, tsunami trough-to-crest heights in Okha (550 km to the north of Mumbai) and in Mormugao (410 km to the south of Mumbai) were 46 cm and 108 cm, respectively. Simulations of a hypothetical MSZ M_w 9.0 earthquake and tsunami, together with the M_w 9.1 Sumatra–Andaman earthquake and tsunami, show that the tsunami heights generated in Mumbai by an MSZ tsunami would be significantly larger than those generated by the 2004 Sumatra–Andaman tsunami. This result indicates that future tsunami hazard mitigation for Mumbai needs to be based on a potential large MSZ earthquake rather than an SASZ earthquake.

Key words: Tsunamis; Indian Ocean; Numerical modelling; Earthquake hazards; Earthquake source observations; Subduction zone processes.

1 INTRODUCTION

The 2004 December Sumatra–Andaman earthquake with M_w 9.1−9.2 (Lay *et al.* 2005; Kanamori 2006; Fujii & Satake 2007) generated the most catastrophic tsunami in recorded history and killed more than 226 000 people (Okal 2015). The tsunami, called hereafter the Indian Ocean (IO) tsunami, devastated 14 countries across the IO including: Indonesia (∼170 000 fatalities, Sibuet *et al.* 2007), Sri Lanka (∼35 000, Tomita *et al.* 2006), India (∼16 000, Maheshwarie *et al.* 2006; Sheth *et al.* 2006; Yeh *et al.* 2006), Thailand (∼8000), Maldives (∼100, Fritz *et al.* 2006) and Somalia (∼300, Fritz & Borrero 2006a). Numerous international field survey teams were formed in the aftermath of the tsunami to record the damage and estimate run-up heights across the Indian Ocean. Borrero *et al.* (2006a) surveyed northern Sumatra, which was severely hit by the near-field tsunami, and reported sustained flow depth of 9 m and run-up of > 30 m. In Sri Lanka, the surveys by Liu *et al.* (2005) and Tomita *et al.* (2006) found run-up heights of up to 13 m, while on the coast of Thailand they were up to 16–20 m (Siripong 2006; Choowong *et al.* 2008; Jankaew *et al.* 2008). By surveying along the coasts of Myanmar, Satake *et al.* (2005) reported tsunami heights of ∼3 m. In Somalia, located ∼5000 km from the epicentre (Fig. 1), the run-up heights were 5−9 m (Fritz & Borrero 2006). Madagascar, an island in the southwestern IO at the distance of ∼6000 km from the epicentre, was also attacked by damaging waves of the 2004 tsunami with maximum run-up of 5.4 m (Okal *et al.* 2006a). The maximum run-up was 3.3 m on the coast of Oman (Okal *et al.* 2006b). Approximately three months after the devastating 2004 December earthquake and tsunami, another destructive M_w 8.6 earthquake occurred on 2005 March 28

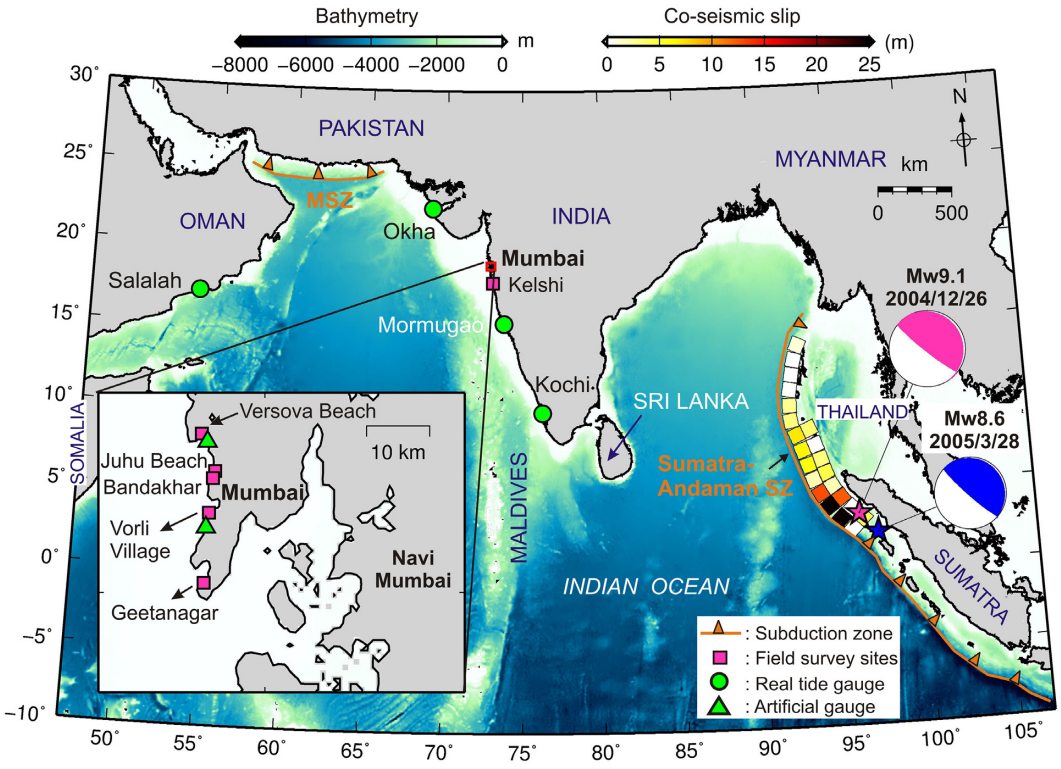

Figure 1. Map of the Indian Ocean showing the source fault of the 2004 IO tsunami and the sites of field works in the area of Mumbai. The red box is enlarged in the inset in the bottom left. Purple and blue stars indicate the epicentres of the M_w 9.1 Sumatra–Andaman earthquake of 2004 December 26 and the M_w 8.6 Nias–Simeulue earthquake of 2005 March 28, respectively. The source mechanisms of these events are from the United States Geological Survey (USGS) earthquake catalogue. The coseismic slip model of the 2004 December earthquake is from Fujii & Satake (2007). MSZ stands for Makran subduction zone.

in a few hundred kilometres to the south from the 2004 epicentre (Fig. 1, blue star), which left a death toll of over 1000 people (Tilmann *et al.* 2010; Borrero *et al.* 2011).

Although many locations have been surveyed following the 2004 tsunami and the tsunami damage and run-ups were thoroughly estimated, these efforts were mainly focused on coasts with extensive fatalities, while many other locations were not surveyed. Among the cities not surveyed was Mumbai (until 1995 known as Bombay), a principal port and economical capital of India on the west coast with a population of more than 12 million. The city has extensive low-lying areas along the coast which accommodate dense populations (De Sherbinin *et al.* 2007). In terms of tsunami hazards, Mumbai is at high risk of tsunamis from two major subduction zones in the IO: the Sumatra–Andaman subduction zone (SASZ), responsible for the 2004 December IO tsunami (*cf.* Lay *et al.* 2005; Titov *et al.* 2005), and the Makran subduction zone (MSZ), responsible for the 1945 November tsunami (Heidarzadeh *et al.* 2008, Fig. 1). In 1945 November, an M_w 8.1 earthquake in the MSZ generated a large tsunami whose trough-to-crest height was ∼50 cm in Mumbai, based on a tide gauge station which recorded the tsunami (Neetu *et al.* 2011; Heidarzadeh & Satake 2015). Among the first steps towards mitigating the tsunami risk for Mumbai and other locations across the IO, is estimation of the effects of the 2004 IO tsunami in this region.

The main purpose of the present research is to understand the effects of major tsunamis on the west coast of India, with particular focus on the area of Mumbai. Our study included three main components: (1) analysis of available tide gauge records of the tsunamis of 2004 December 26 and 2005 March 28 at the coast of west India and adjacent regions; (2) field survey of the coastal region of Mumbai to estimate run-up heights and damage caused by the 2004 December IO tsunami; and (3) numerical simulation of the tsunami effects in Mumbai produced by the actual 2004 IO tsunami and by a tsunami generated by a hypothetical M9 earthquake in the MSZ. For the numerical modelling of the 2004 tsunami we used the validated source model of Fujii & Satake (2007) and studied propagation and coastal amplifications of tsunami waves in the northwestern IO, focusing on the area in and around Mumbai. Similar modelling was also done for a potential M9 MSZ earthquake and tsunami.

2 DATA AND METHODS

The data used in this study are: actual tide gauge records of the 2004 December IO and 2005 March Nias–Simeulue tsunamis, bathymetric data for tsunami simulations and observational data obtained through field surveys. Tide gauge records of the 2004 tsunami are from three stations along the west coast of India (Kochi, Mormugao and Okha) and one station on the coast of Oman (Salalah, Fig. 1). For the 2005 tsunami only the record at Salalah was available. Also, although the Mumbai tide gauge station has been operational since 1878, the 2004 tsunami record at this station was unavailable (Rabinovich & Thomson 2007). That is why, to examine the tsunami hazard in the Northwest IO during this event, we used the data from the previously-mentioned stations. The sampling intervals of the records are: 4 min (Salalah), 5 min (Mormugao) and 6 min (Kochi and Okha). The data were provided by the Survey of India, Delhi (India), and the National Institute of Oceanography, Goa (India). The original analog records at Okha and Mormugao were digitized with indicated sampling intervals, while the other two records were digital. We applied these records to study the tsunami hazard in

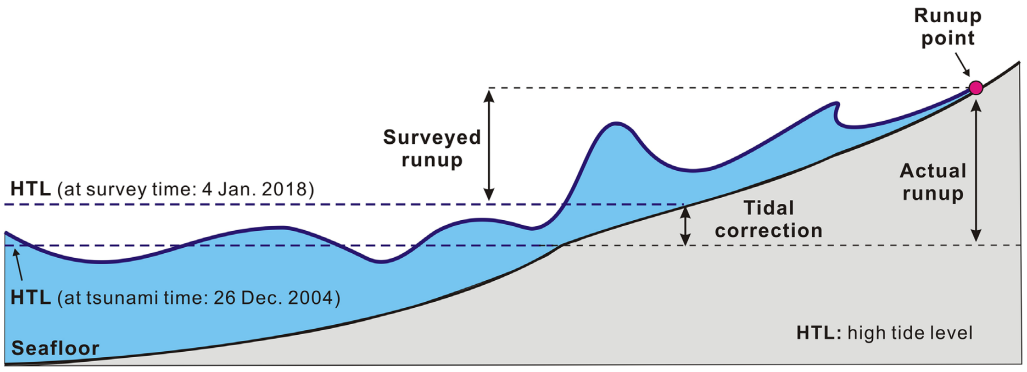

Figure 2. Sketch showing the tidal corrections for the measured run-up heights in order to obtain the actual run-up heights of the 2004 IO tsunami. HTL = high tide level.

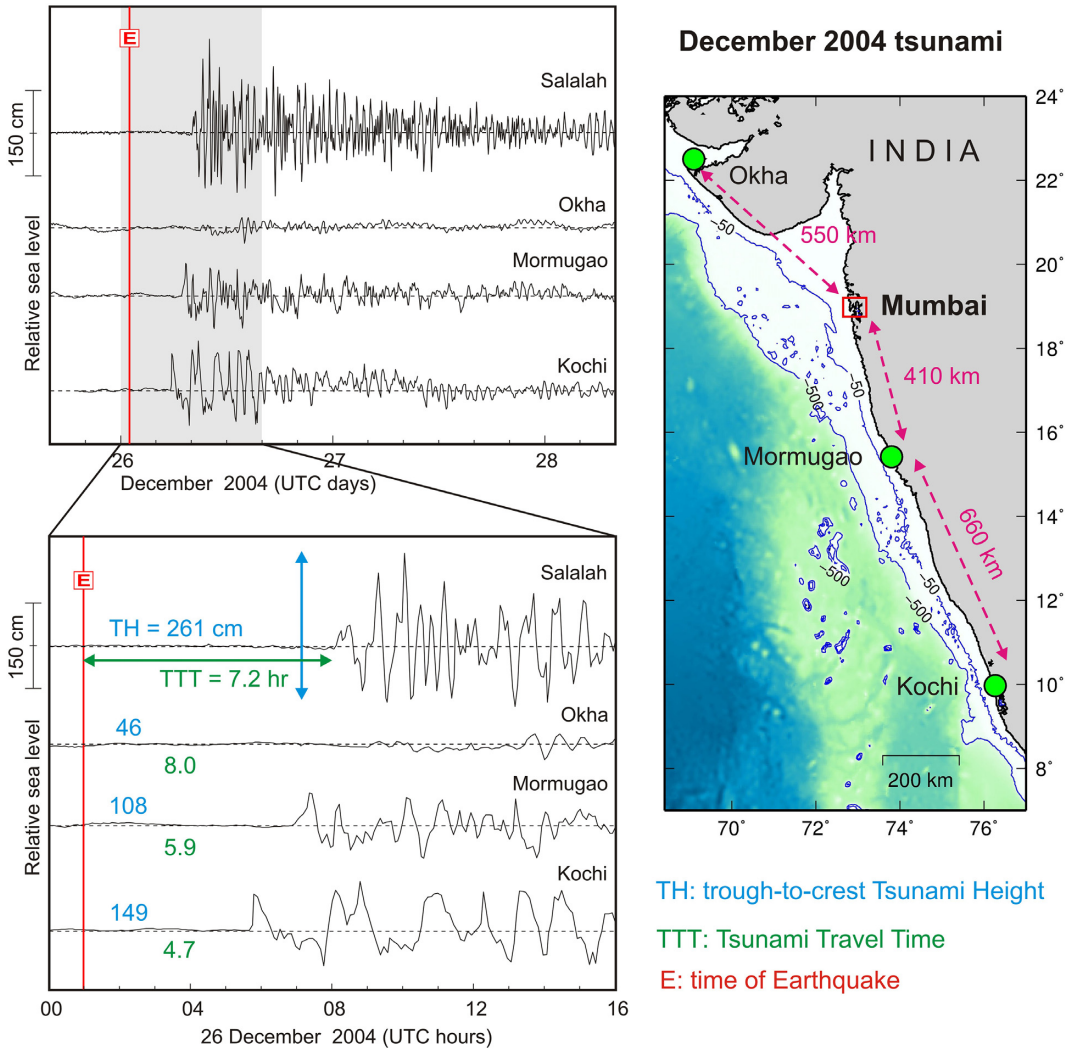

Figure 3. Tide gauge records of the 2004 December Indian Ocean tsunami on the west coast of India and at Salalah (Oman). TTT = tsunami traveltime (in hours) and TH = trough-to-crest tsunami height (in cm). The letter 'E' indicates the time of the earthquake origin time.

Mumbai and nearby regions. Previously, the 2004 data from these and other IO stations were examined by Nagarajan *et al.* (2006) and Rabinovich & Thomson (2007). We used the least squares method of harmonic analysis to estimate the tidal signal (*cf.* Rabinovich *et al.* 2006; Rabinovich & Thomson 2007) and removed it from the original time-series. The residual (de-tided) time-series enabled us to extract the tsunami waveforms.

To collect information about the 2004 run-up heights and local damage, we interviewed eyewitnesses of the 2004 IO tsunami and measured the run-up heights, where this was possible, during 2018

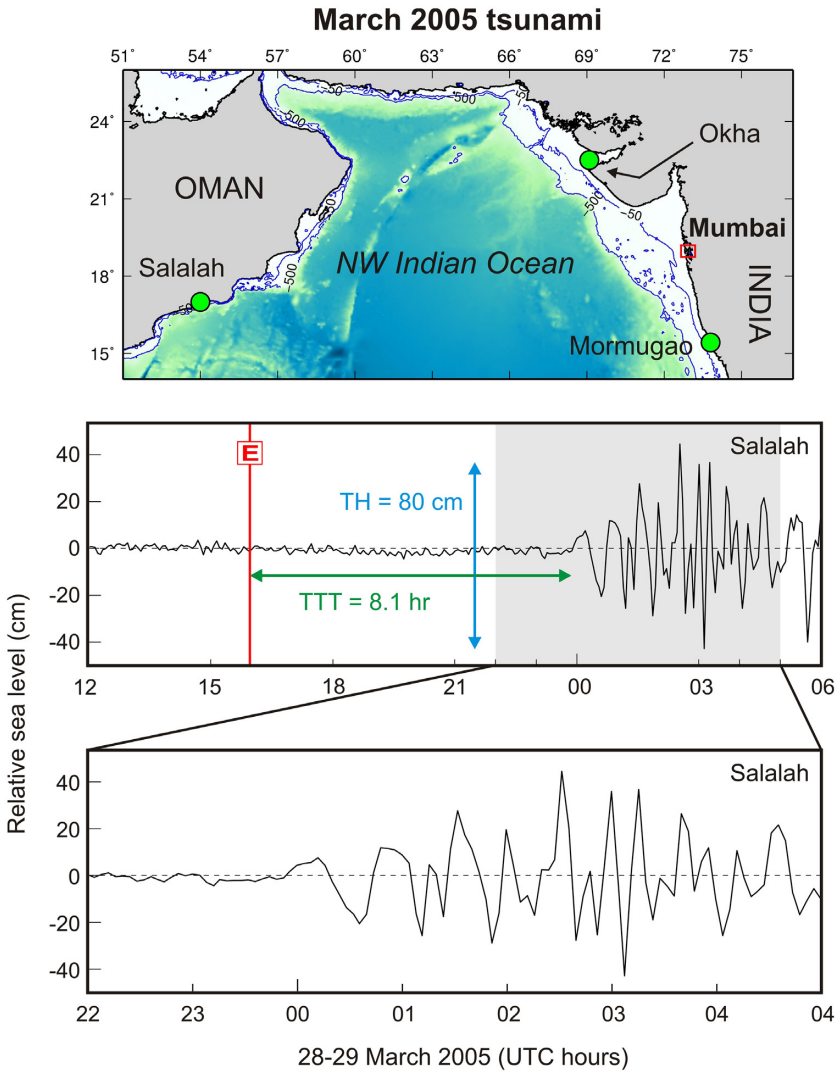

Figure 4. Tide gauge record of the 2005 March tsunami as recorded at Salalah (Oman). TTT = tsunami traveltime (in hours) and TH = trough-to-crest tsunami height (in cm). The letter 'E' indicates the time of the earthquake origin time.

January 1−5. Two Mumbai local officers from the Disaster Management Unit of Mumbai accompanied us in the field survey, helping us in finding appropriate locations and eyewitnesses. As the event had occurred 13 yrs before the time of the survey, we interviewed only individuals older than 34 yrs, that is those who were older than 20 yr at the time of the event are able to recall the event appropriately, giving essential details. We surveyed six locations in the area of Mumbai (Fig. 1) and measured the run-up heights using a TruPulse 200 laser range-finder manufactured by Laser Technology Inc. (http://www.lasertech.com/TruPulse-200-B-Rangefinder.aspx) assisted with a reflector. A hand-held Garmin model Montana 680t GPS (https://buy.garmin.com/en-US/US/p/523677) was applied to register the exact positions of our measurements. All run-up estimations were done relative to the high tide level (Pugh & Woodworth 2014); then were corrected according to the high tide level at the time of the event (i.e. 2004 December 26, Fig. 2). To evaluate high tide levels on 2004 December 26, we applied the data from the online tidal prediction provider WorldTides (https://www.worldtides.info/home). Based on the previous experience of field surveys of this type, we estimated the errors associated with the run-up measurements to be up to ± 30 cm including device measurement errors, witnesses' judgment errors and slope of the beach (Synolakis & Okal 2005; Heidarzadeh *et al.* 2018a; Omira *et al.* 2019).

The numerical simulations were conducted using the computational package JAGURS (https://github.com/jagurs-admin/jagurs , Baba et al., 2014, 2015), allowing solving of Linear/Nonlinear Shallow-Water/Boussinesq Equations for a uniform or nested grid system. JAGURS has options to consider the effects of elastic deformation of the Earth during transoceanic propagation of tsunamis, as well as the vertical profile of sea water density stratification (*cf.* Watada *et al.* 2014). As transoceanic tsunamis experience dispersion during their long-distance travel paths, it is recommended to use dispersive models for their numerical simulation (Løvholt *et al.* 2012; Saito *et al.* 2014; Heidarzadeh *et al.* 2014). A two-level nested grid system with grid resolutions of 45 and 5 arcsec for the entire IO and the areas around tide gauges, respectively, was employed in our numerical modelling efforts. Although it is desirable to use high-resolution bathymetry data with a grid resolution of 10–20 m for inundation modelling, the experience shows that a grid

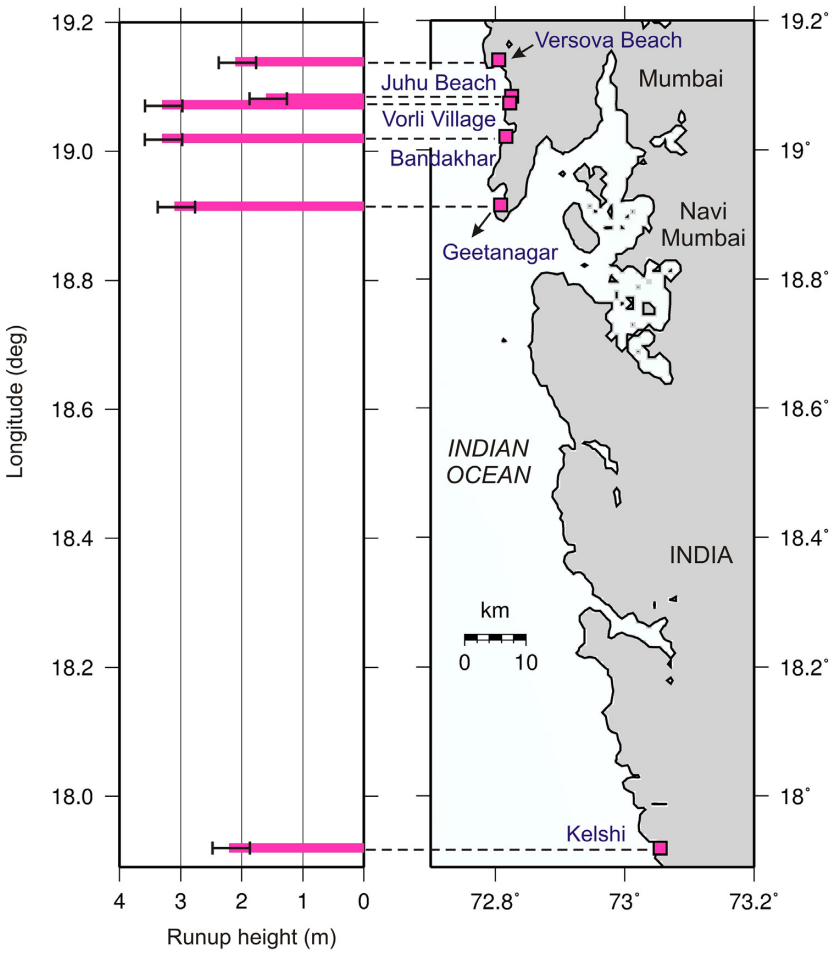

Figure 5. Results of the field survey of the 2004 IO tsunami (pink solid bars) at six coastal locations in the Mumbai area, west coast of India, with indicated uncertainty levels of ± 0.3 m.

resolution of 100–200 m (3.2–6.4 arcsec) gives satisfactory results (e.g. Borrero *et al.* 2006b; Heidarzadeh *et al.* 2009). Here, the bathymetric data are based on the 30 arcsec grid of the General Bathymetric Charts of the Oceans (Weatherall *et al.* 2015). This bathymetric grid was resampled to produce the nested grids used for detailed tsunami simulations for the area of Mumbai. As Mumbai is located thousands of kilometres away from the source region of the 2004 IO tsunami, the tsunami simulation was of transoceanic type. Therefore, we considered all transoceanic effects for the tsunami modelling including, nonlinear dispersion, elastic loading, sea water compressibility and density stratification. In accordance with the CFL (Courant, Friedrichs and Lewy) criterion for the stability of numerical simulations, the time-step was chosen to be 1.0 s and the total simulation time was 24 hr. The Fujii & Satake's (2007) source model, which was applied for simulation of the 2004 IO tsunami, includes 22 subfaults, each having dimensions of 100 km (length) × 100 km (width) and slip values up to 25 m (Fig. 1). The M9 earthquake and consequent tsunami in the MSZ is based on the hypothetical worst-case scenario previously proposed by Heidarzadeh *et al.* (2009, scenario-2 in Table 2 of Heidarzadeh *et al.* 2009) that involves two subfaults with a total length of 900 km, width of 150 km and uniform slip of 25 m. Other source parameters are: depth, 25 km; rake angle, 90°; strike angles of the two fault segments 265° and 280°. The two M9 earthquakes in MSZ and SASZ have certain differences: the SASZ M9 has a heterogeneous slip distribution (Fig. 1), while that of MSZ M9 comes with uniform slip; the source length of the SASZ M9 event is ∼1100 km, whereas it is ∼900 km for the MSZ M9 earthquake. For both events, the crustal coseismic deformation, which is used as the initial condition for tsunami simulations, was calculated based on analytical equations of Okada (1985).

3 SEA LEVEL RECORDS OF THE 2004 AND 2005 TSUNAMIS

In the NW IO, where Mumbai is located, the 2004 IO tsunami was recorded by four tide gauges (Rabinovich & Thomson 2007). We do not have an actual tsunami record in Mumbai, but the available four records (Fig. 3) give insights into the expected parameters of the 2004 IO tsunami around Mumbai. Mumbai is located between the stations of Mormugao and Okha with respective distances of 410 and 550 km from each. The region offshore of the west coast of India is characterized by a wide continental shelf with relatively shallow water depths of < 500 m; the width of this shelf is 100−400 km and increases towards the north (Fig. 3). As a result of this extended shallow shelf, tsunami waves propagate comparatively slowly, with the wave speed of $C = \sqrt{gd} \approx 100$–$150$ km h^{-1}, where g is gravity acceleration and d is the water depth. Also this extended shallow shelf is responsible for the generation of edge waves trapped along the coastline (e.g. Neetu *et al.* 2011; Satake *et al.* 2020).

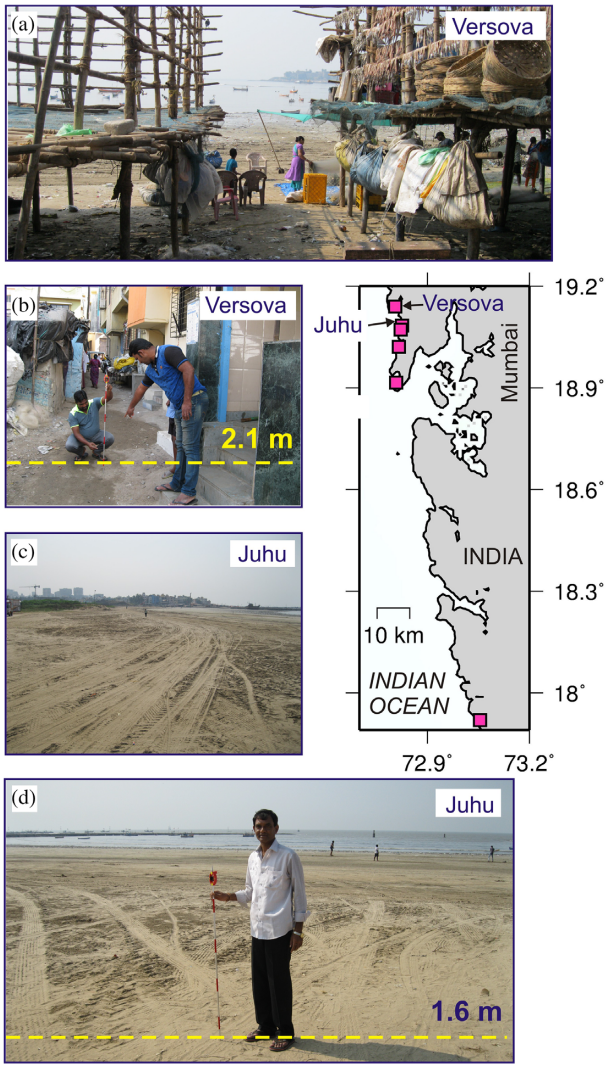

Figure 6. The 2004 tsunami run-up heights and photos of the respective locations in Versova and Juhu, Mumbai. Survey was conducted in 2018 January.

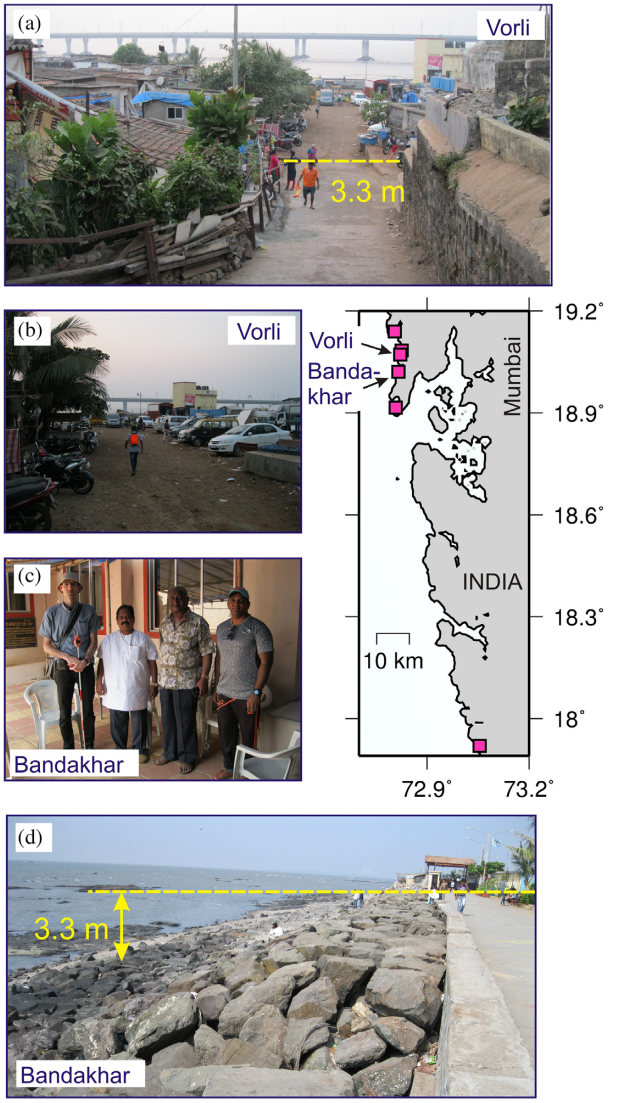

Figure 7. The 2004 tsunami runup heights and photos of the respective locations in Vorli and Bandakhar, Mumbai. Survey was conducted in January 2018.

According to Rabinovich & Thomson (2007), based on the analysis of tide gauge records, tsunami travel times (TTT) to Kochi, Mormugao and Okha are 4 hr 09 min, 5 hr 54 min and 8 hr 04 min, respectively, with corresponding trough-to-crest tsunami heights (TH) of 149, 108 and 46 cm at these stations (Fig. 3). It can be seen that the TH decreases as the tsunami travels northward from Kochi to Okha. The TH decay rate can be approximated as 0.1 cm km^{-1}. Therefore, the 2004 IO TH and TTT at Mumbai can be approximated as TH ∼77 cm (i.e. average value of 46 and 108 cm) and TTT∼7 hr (i.e. average value of 5.9 and 8.0 hr), respectively. In fact, TTTs and wave heights at tide gauge locations strongly depend on actual regional bathymetry and resonant properties of local topography in the specific bays and harbours where tide gauges are installed. Therefore, the TTT and TH values estimated here for Mumbai should be considered as approximate. More precise estimates can be obtained numerically as is discussed in Section 5. Fig. 4 reveals that the 2005 March SASZ tsunami produced a wave height of 80 cm at Salalah, that is 3.3 times smaller than the 2004 December SASZ tsunami. It appears that the 2004 tsunami can be considered as a 'worst-case scenario' for the SASZ region, although other 'worst-case scenarios' were also considered for the SASZ (e.g. Okal & Synolakis 2008; Hebert & Schindele 2015).

Tsunami run-up (R) on a particular coast can be approximated based on trough-to-crest tide gauge heights (H_{tg}) at the corresponding location. Soloviev (1978) proposed a ratio:

$$R \sim 1.4\, H_{tg}, \quad (1)$$

Eq. (1) gives a very general estimate of R along the coast because run-up heights can significantly vary from one coastal point to another due to the coastal geometry, the bathymetry of the adjacent coastal zone, slope angle and roughness of the beach (e.g. presence of buildings and vegetation). The estimations based on equation (1) should be considered as very preliminary; updating of this equation for a specific region can be based on available information from large tsunamis and on taking into account local phenomena such as harbour resonance and edge waves. By applying the Eq. (1) and assuming that H_{tg} ∼77 cm in Mumbai, the run-up of the 2004 IO tsunami in the Mumbai region should be ∼1.1 m. However, for particular events and specific regions, the run-up height could be several times larger than the tide gauge heights. For example, the 2004 tide

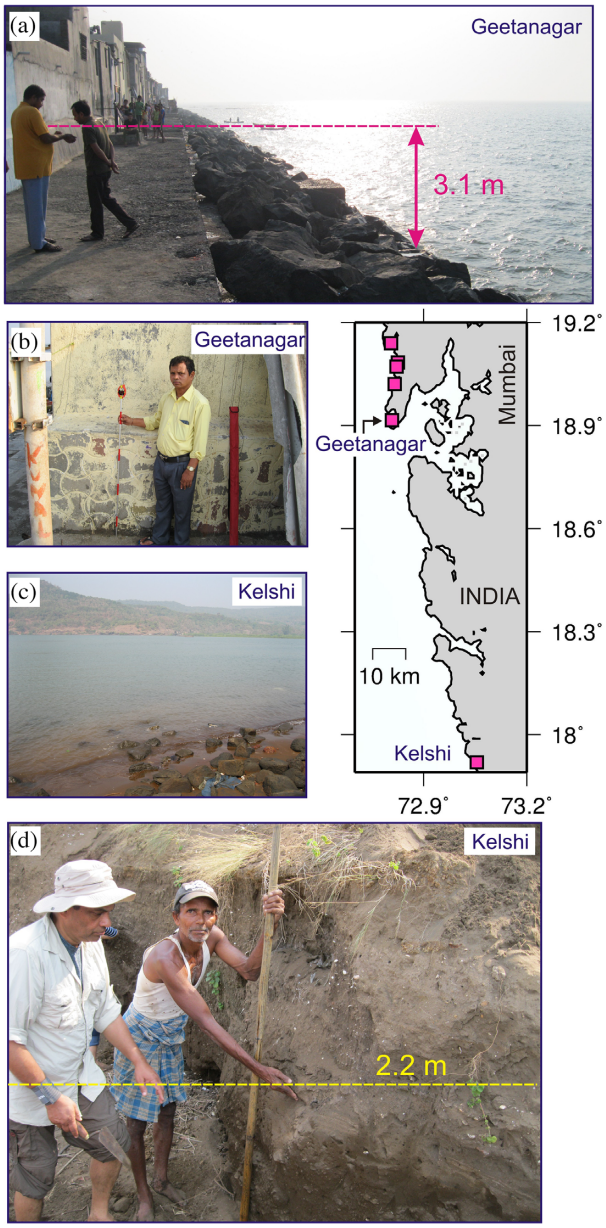

Figure 8. The 2004 tsunami runup heights and photos of the respective locations in Geetanagar and Kelshi. Survey was conducted in 2018 January.

gauge tsunami heights along the coast of Thailand were 0.6−2.2 m (Rabinovich & Thomson 2007), while field survey measured runups were 2.8−11.9 m (Siripong 2006). For the 2018 December Sunda Strait (Anak) tsunami (Indonesia), the run-up heights were up to 4.8 times larger than tide gauge tsunami heights (Heidarzadeh *et al.* 2020).

4 TSUNAMI RUN-UP FIELD SURVEYS ON THE COAST OF MUMBAI

The 2004 December 26 Sumatra–Andaman M_w 9.1 earthquake occurred at 0:58:53 UTC (Lay *et al.* 2005). Given a ∼7 hr of TTT, the local time in Mumbai was approximately 13:30, when the wave arrived. Therefore, the tsunami came to the Mumbai region around the middle of the day; this was probably the reason why the memories of the tsunami run-up heights and watermarks were relatively clear for most of the eyewitnesses interviewed during our field survey. Furthermore, the global impact of the tsunami (Titov *et al.* 2005; Synolakis & Bernard 2006; Satake 2014) and the international coverage in the news, made the event highly memorable to most people. Fig. 5 and Table 1 present the results of run-up survey at all six locations in the Mumbai region, while Figs 6–8 give detailed information and photos for the survey points. The measured run-up heights were in the range of 1.6−3.3 m. Below, each run-up location is discussed in detail.

4.1 Versova Beach

Versova is a fishing community near Mumbai on the west coast of India (Figs 6a and b). Here, we interviewed several locals, including Vijay, 35-yr-old fisherman. According to eyewitness reports, the inundation limit was evident and was pointed out to us (Figs 6a and b). We estimated the run-up height of 2.1 ± 0.3 m. As seen in Fig. 6, Versova is a low-lying area, which allows the tsunami to inundate deeply onto the beach without gaining much height (e.g. Tsuji *et al.* 2011; Mori *et al.* 2012).

4.2 Juhu Beach

Juhu Beach is also a low-lying flat beach, similar to Versova (Figs 6c and d). We interviewed Prabhakar, a 56-yr-old local fisherman, who observed a water level raise and inundation; he understood that something unusual was going on. According to his report, several fishing boats were washed away from the shore, but he did not notice any significant damage to the boats and coastal facilities. With his guidance, we recorded a wave run-up height of 1.6 ± 0.3 m (Figs 6c and d).

4.3 Vorli Village

Vorli Village is a fishing community with a steep-slope coast (Figs 7a and b). This location is in significant contrast with the coast at Versosa and Juhu beaches that have gentle beach slopes. Here, we interviewed a fisherman in his early 50s who showed us the 2004 inundation limit. According to this fisherman, the 2004 tsunami run-up was unique; he had never seen such a large inundation and run-up in the past. Our estimate of a run-up height at this site was 3.3 ± 0.3 m (Figs 7a and b).

In comparison to the run-up heights at the flat beaches in Versosa and Juhu (1.6−2.1 m; Fig. 6), the run-up height at Vorli was considerably larger (3.3 m; Figs 7a and b). This can be directly attributed to the much steeper beach slope at the latter site. According to the results of post-tsunami field surveys in Japan after the 2011 Tohoku tsunami (Mori *et al.* 2012), tsunami energy is transferred into large run-up heights with relatively short inundation distances at steep-slope beaches and, vice versa, is converted into low run-up heights and long inundation distances at gently sloped beaches. Such behaviour was also observed recently during the 2018 Anak Krakatau volcanic tsunami where larger run-up heights were found along the cliff-type coastlines and significantly smaller run-ups along the flat-type beaches (Muhari *et al.* 2019; Heidarzadeh *et al.* 2020). Another factor controlling run-up is wave focusing due to submarine bathymetric features.

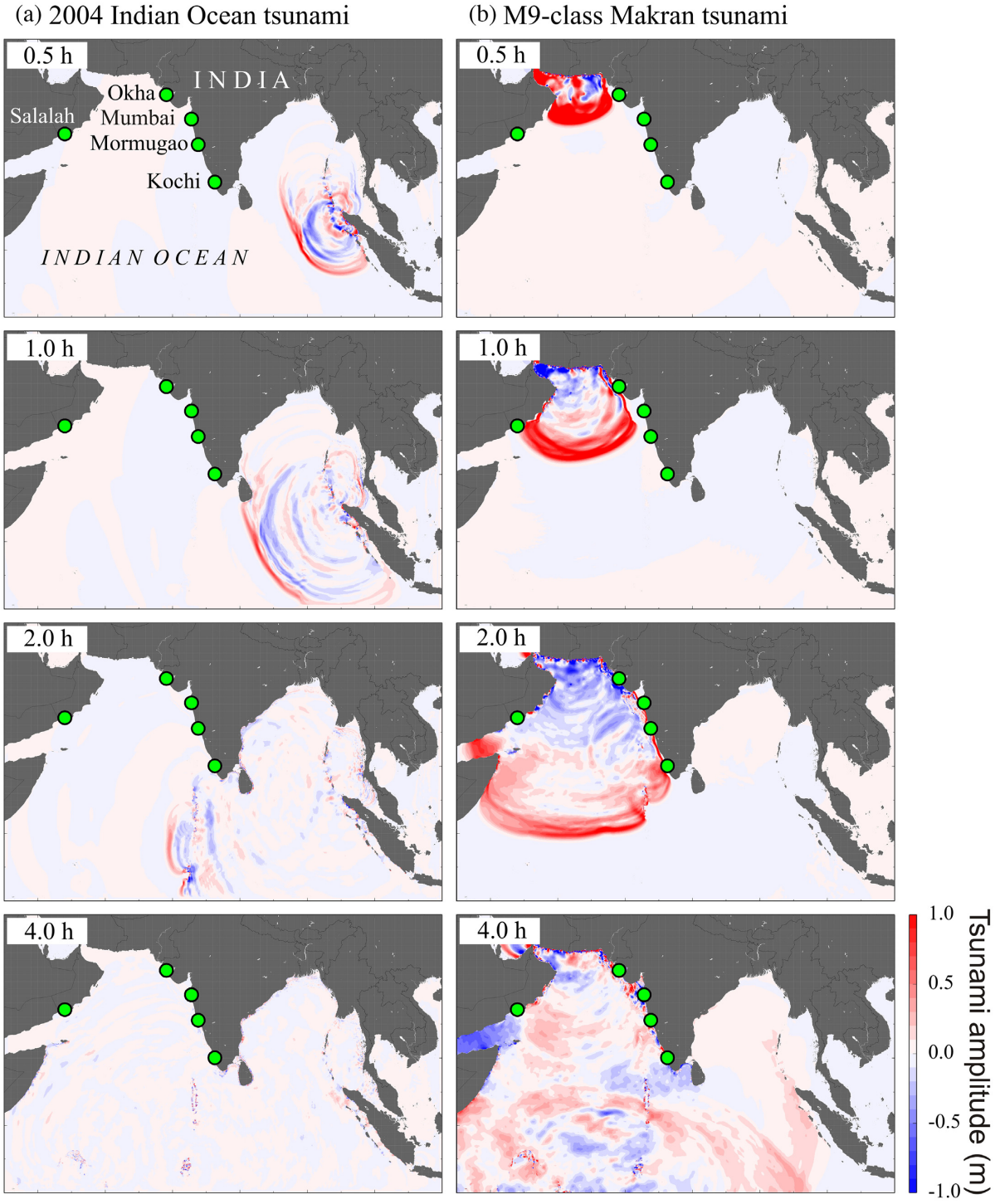

Figure 9. Snapshots of tsunami simulations for (a) the real 2004 IO tsunami and (b) a hypothetical M9 earthquake in the MSZ. The green circles show locations of tide gauges. The tide gauge station in Mumbai is a virtual one.

4.4 Bandakhar

Similar to Vorli Beach, the beach in Bandakhar is also relatively steep (Figs 7c and d). We interviewed two residents living at a house at a distance of approximately 35 m from the shoreline (Fig. 7c). The main tsunami feature here, according to both individuals, was the inundation of the nearby coastal road (Fig. 7d) that had never occurred before. The tsunami run-up height was estimated at Bandakhar to be 3.3 ± 0.3 m.

4.5 Geetanagar

The beach in Geetanagar has a steep slope and is elevated (Figs 8a and b). A resident in his 50s, Randas, was interviewed here and said that the 2004 IO tsunami was the largest event he had ever experienced. At the time of the tsunami, this eyewitness had been living at this coast for several decades. He showed us the inundation level (Fig. 8b), which yielded a run-up height of 3.1 ± 0.3 m at this location.

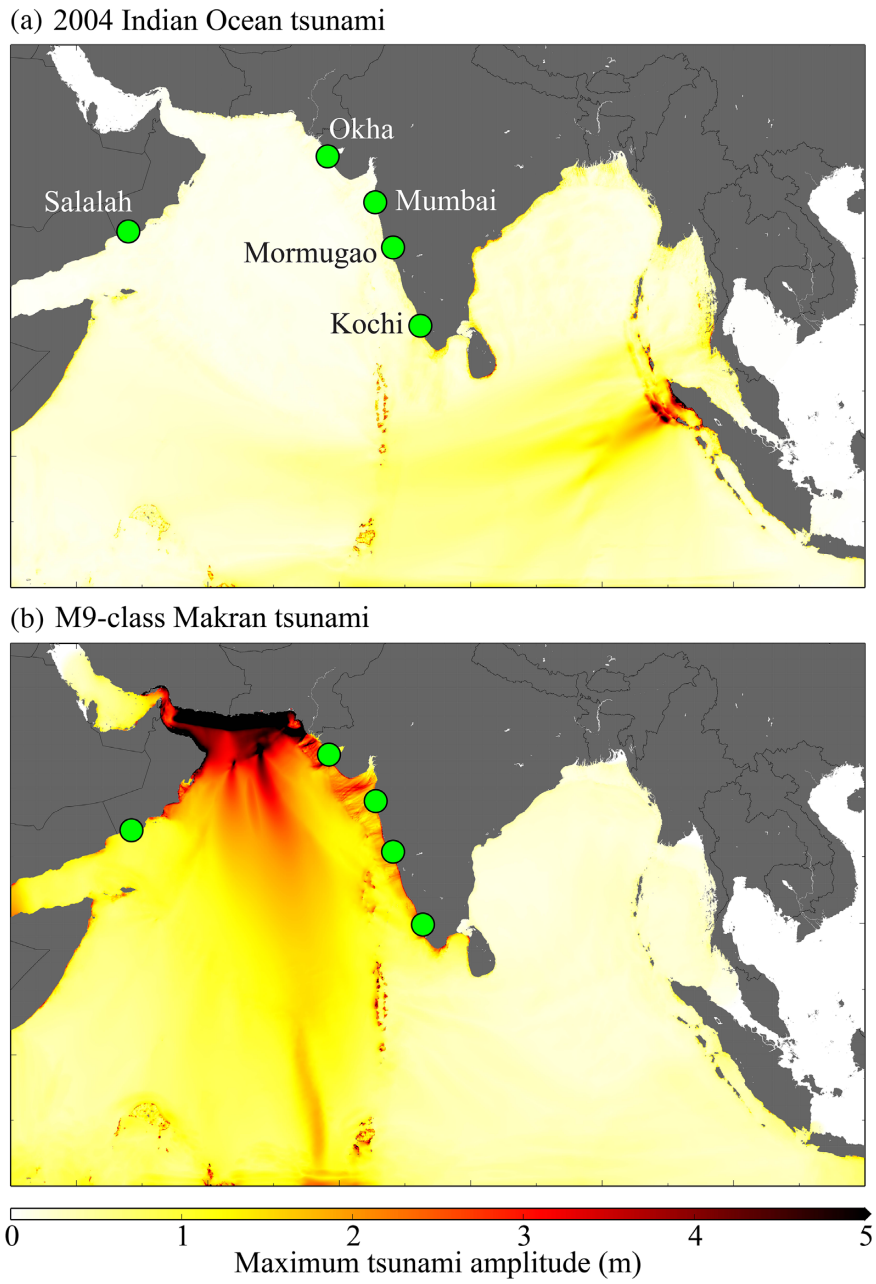

Figure 10. The maximum simulated tsunami wave heights during 24 hr of tsunami simulations for (a) the real 2004 IO tsunami and (b) a hypothetical M9 earthquake in the MSZ. The green circles show locations of tide gauges. The tide gauge station in Mumbai is a virtual one.

4.6 Kelshi

Kelshi is a small fishing village, located ~160 km to the south of Mumbai, around a coastal lagoon (Figs 8c and d). Several locals were interviewed here; among them were two fishermen and a security guard familiar with the coastline. According to their observations, the 2004 IO tsunami did not make notable damage here. The run-up height was 2.2 ± 0.3 m.

5 NUMERICAL SIMULATIONS

The main purpose of tsunami simulations was to examine maximum potential tsunami wave heights in the Mumbai region from the worst-case scenarios of tsunamis generated in the MSZ and SASZ. The simulations results for the MSZ and SASZ M9 earthquakes/tsunamis, including the real 2004 tsunami and a hypothetical MSZ tsunami, are presented in Figs 9–11. According to snapshots (Fig. 9), the SASZ tsunami is reflected and diffracted from Sri Lanka and the southern tip of India; as a result, only a fraction of the tsunami energy penetrated into the NW IO and the Mumbai area. In contrast, the MSZ tsunami directly hits the west coast of India, including Mumbai. The maximum tsunami wave heights (Fig. 10) reveal that the main branch of the SASZ energy is directed towards the west and southwest; in agreement with the modelling results of Titov *et al.* (2005) and Kowalik *et al.* (2007). In contrast, our simulation results demonstrate that the Makran tsunamis attack

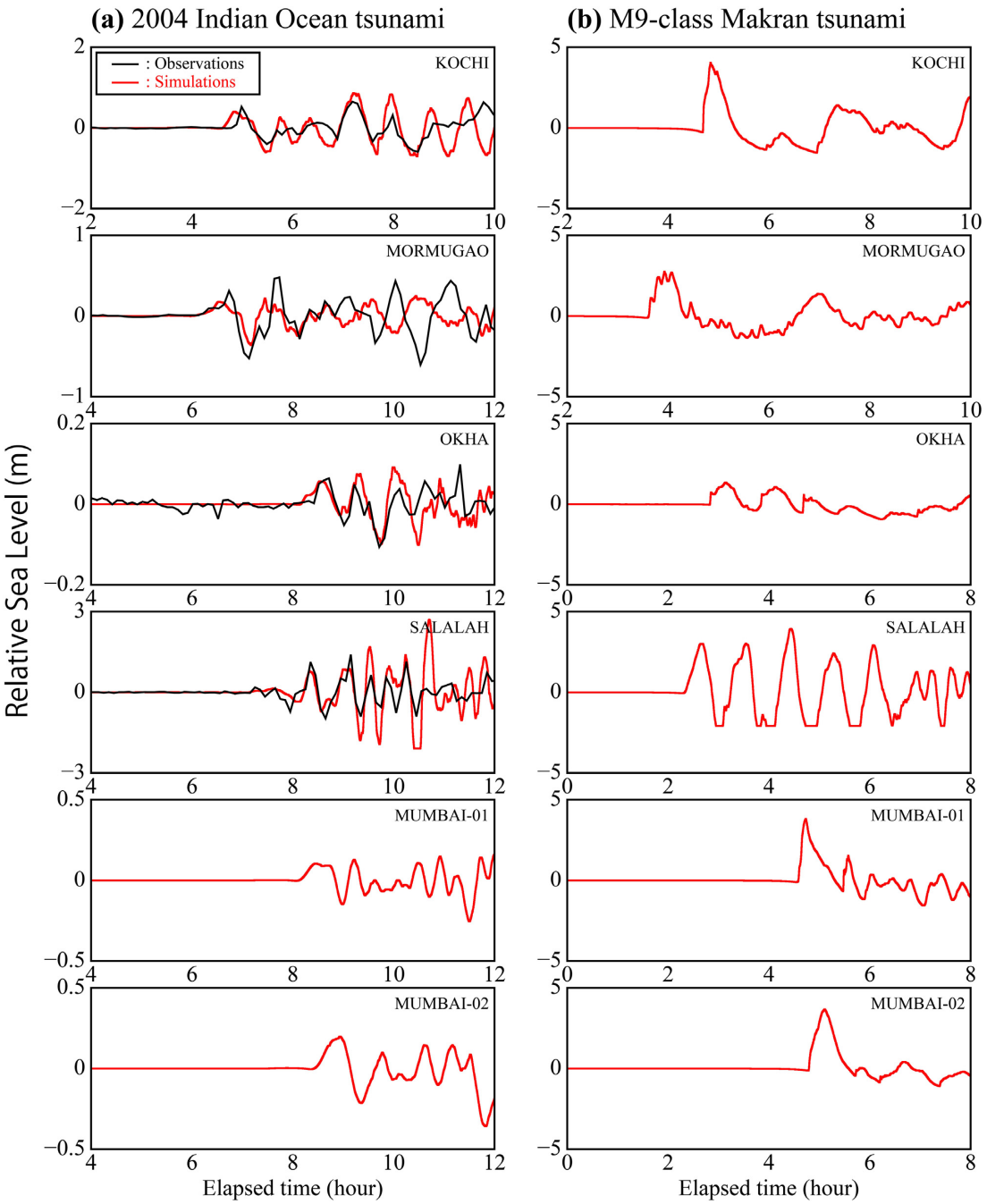

Figure 11. Observed (black) and simulated (red) waveforms for (a) the real 2004 IO tsunami and (b) a hypothetical M9 earthquake in the MSZ. There are no real observations of the 2004 IO tsunami in Mumbai and thus both Mumbai gauges in the panel 'a' are virtual gauges (see Fig. 1 for locations of these gauges). The simulated waveforms at Kochi, Okha and Salalah are time-shifted by 10, 24 and 2 min, respectively, to match the observations. The Mormugao simulation is shifted 1 d and 65 min to match the observations; it appears that there was a clock error in the Mormugao data.

directly the area of Mumbai. Therefore, in terms of possible hazardous effects, Makran tsunamis appear to be much more dangerous for Mumbai than Sumatra–Andaman tsunamis.

The actual tide gauge records of the 2004 IO tsunami, in general, are in good agreement with the simulated tsunami waveforms computed for a two-level nested grid system (Fig. 11). However, there were little time-shifts of simulated waveforms in comparison with observations. Time delays of observed tsunami records relative to simulated waveforms for far-field events have been previously reported by several authors (Rabinovich et al. 2011b, 2013; Watada *et al.* 2014; Allgeyer & Cummins 2014; Heidarzadeh *et al.* 2018b). The best agreement between modelling and observations was achieved after making some time corrections (Fig. 11). It can be seen that the character of the waveform varies from one station to another. For example, the 2004 waveform at Kochi lasts for more than 5 hr, while the Makran M9's waveform shows a large initial peak followed by a rapid decay (Fig. 11). Similar behaviour can be seen at Mormugao and Mumbai. These results are in good agreement with Rabinovich *et al.* (2011a) who showed that the near-field tsunamis decay fast, while the far-field tsunamis decay slower.

Table 1. Results of run-up height surveys of the 2004 IO tsunami at six coastal locations in Mumbai.

No.	Location	Longitude (°E)	Latitude (°N)	Measured run-up height (m)	Date and time of survey (local time)	Tide correction (m)	Run-up (m)
1	Versova Beach	72.8055	19.1386	1.6	2018 Jan 6 (12:00)	+0.5	2.1 ± 0.3
2	Juhu Beach	72.8251	19.0832	1.1	2018 Jan 6 (14:00)	+0.5	1.6 ± 0.3
3	Vorli Village	72.8161	19.0198	2.7	2018 Jan 5 (17:30)	+0.6	3.3 ± 0.3
4	Bandakhar	72.8219	19.0718	2.8	2018 Jan 6 (16:00)	+0.5	3.3 ± 0.3
5	Geetanagar	72.8084	18.9145	2.5	2018 Jan 5 (16:00)	+0.6	3.1 ± 0.3
6	Kelshi	73.0548	17.9203	1.8	2018 Jan 3 (16:00)	+0.4	2.2 ± 0.3
	Mean runup						2.6 ± 0.3

The validated 2004 IO tsunami simulated waveforms were used to estimate tsunami heights and periods in the Mumbai area. According to Fig. 11(a), the trough-to-crest wave heights (H_{tg}) at the two virtual Mumbai gauge locations were 0.3−0.45 m. The evaluated period of the leading tsunami wave was approximately 45−57 min, which is close to the estimates of Rabinovich & Thomson (2007) and Rabinovich *et al.* (2011a) of the dominant period of the 2004 IO tsunami. Assuming the run-up height of $R = 2.6 \pm 0.3$ m from our survey (Table 1), the ratio of R/H_{tg} becomes ∼5−9 which is significantly larger than the ratio of 1.4 proposed by Soloviev (1978). The substantially larger R/H_{tg} ratios appear to be a typical feature of tsunamis produced by major M9 earthquakes. We note that the R/H_{tg} ratio is strongly affected by the slope angle and the roughness of the coast, as well as by the bathymetry, wavelength and type of tsunami.

While simulated trough-to-crest wave heights of the 2004 IO tsunami for tide gauge sites in the NW IO are less than 2.6 m, those from a M9 earthquake in the Makran zone exceed 6 m (Fig. 11). In particular, at two simulated Mumbai virtual gauge locations, an MSZ M9 earthquake produces trough-to-crest wave heights of 4.8 m, while they are less than 0.45 m from an M9 SASZ earthquake, that is approximately 11 times smaller. For the Mumbai region, the minimum and maximum values of the R/H_{tg} ratio can be considered between 1.4 (given by Soloviev 1978) and 5 (given by our numerical analysis), respectively. By assuming R/H_{tg} ratio of 1.4−5, we can roughly evaluate the run-up heights of a potential MSZ M9 event in the range of 7−24 m in the Mumbai area. For this reason, future tsunami hazard mitigation and development of tsunami countermeasures in Mumbai should be based on potential M9 earthquakes in the Makran zone rather than on the Sumatra–Andaman earthquakes.

6 CONCLUSIONS

A field survey of the 2004 IO tsunami was conducted in the area of Mumbai (India) in 2018 January, aiming at recording tsunami run-up heights based on eyewitness reports. The survey results were supplemented by tide gauge data analysis of the 2004 tsunami records and numerical simulations of worst-case scenarios of tsunamis generated in the MSZ and SASZ. Main findings are:

(i) Based on the observed 2004 tsunami wave heights at Okha (46 cm), located 550 km northward from Mumbai, and at Mormugao (108 cm), which is 410 km to the south of Mumbai, we roughly estimated trough-to-crest wave heights at Mumbai to be ∼70 cm.

(ii) The field survey evaluated run-up heights of the 2004 IO tsunami in the Mumbai region were in the range of 1.6−3.3 m: the tsunami run-up heights along steeply sloping beaches were in the range of 3.1−3.3 m and were 1.6−2.2 m along gently sloping beaches.

(iii) Numerical simulations of M9 earthquakes and tsunamis in the MSZ and SASZ revealed that, in terms of tsunami energy's directivity, the Makran tsunamis directly hit Mumbai, while the Sumatra–Andaman tsunamis are diffracted and reflected by Sri Lanka and the southern tip of India. For this reason, the Makran tsunamis were found to be much more dangerous for Mumbai than the Sumatra–Andaman tsunamis.

(iv) According to the results of our numerical modelling, for similar M9 earthquakes in the MSZ and SASZ, the run-up heights in the Mumbai region from the Makran tsunamis appear to be significantly higher than those from the Sumatra–Andaman tsunami. Therefore, the tsunami hazard mitigation for Mumbai needs to be based on potential major Makran earthquakes rather than on Sumatra–Andaman earthquakes.

ACKNOWLEDGEMENTS

The tide gauge data used in this research were provided by the Survey of India, Delhi (India), and the National Institute of Oceanography, Goa (India). We used the GMT software by Wessel & Smith (1998) for drafting the figures. MH is grateful to Jaishri Sanwal (Jawaharlal Nehru Centre for Advanced Scientific Research, Bangalore, India), Kusala Rajendran (Indian Institute of Science, Bangalore, India) and the staff at the Navi Mumbai Municipal Corporation (NMMC). A special acknowledgement to Vrindha Nath (NMMC), and to the Disaster Management Unit of Mumbai for helping with the field survey in the Mumbai region and for the fruitful discussions. The authors gratefully acknowledge Fred Stephenson (Institute of Ocean Sciences, Sidney, BC, Canada) for valuable comments and suggestions. The manuscript benefitted from constructive review comments from Prof Gabi Laske (the Editor) and two anonymous reviewers for which we are sincerely thankful. MH is grateful to Prof Serge Guillas (University College London, UK) for valuable discussions and encouragements. This research was funded by the Natural Environment Research Council (NERC) of the United Kingdom; contract number NE/P016367/1. MH was also funded by the Royal Society, the United Kingdom (grant number CHL/R1/180173). CPR acknowledges funding from the Board of Research in Nuclear Sciences, Department of Atomic Energy, Government of India. For AR, this work was partially supported by the Russian State Assignment of IORAS number 0149-2019-0005. The authors declare that they have no competing interests regarding the work presented in this paper.

REFERENCES

Allgeyer, S. & Cummins, P., 2014. Numerical tsunami simulation including elastic loading and seawater density stratification, *Geophys. Res. Lett.,* **41**(7), 2368–2375.

Baba, T., Takahashi, N. & Kaneda, Y., 2014. Near-field tsunami amplification factors in the Kii Peninsula, Japan for Dense Oceanfloor Network for Earthquakes and Tsunamis (DONET), *Mar. Geophys. Res.,* **35**(3), 319–325.

Baba, T., Takahashi, N., Kaneda, Y., Ando, K., Matsuoka, D. & Kato, K., 2015. Parallel implementation of dispersive tsunami wave modeling with a nesting algorithm for the 2011 Tohoku tsunami, *Pure appl. Geophys.,* **172**(12), 3455–3472.

Borrero, J.C., Synolakis, C.E. & Fritz, H., 2006a. Northern Sumatra field survey after the December 2004 Great Sumatra earthquake and Indian Ocean tsunami, *Earthq. Spectra,* **22**(S3), 93–104.

Borrero, J.C., Sieh, K., Chlieh, M. & Synolakis, C.E., 2006b. Tsunami inundation modeling for western Sumatra. *Proc. Natl. Acad. Sci.,* **103**(52), 19673–19677.

Borrero, J.C. *et al.*, 2011. Field survey of the March 28, 2005 Nias-Simeulue earthquake and tsunami, *Pure appl. Geophys.,* **168**(6–7), 1075–1088.

Choowong, M. *et al.*, 2008. 2004 Indian Ocean tsunami inflow and outflow at Phuket, Thailand, *Mar. Geol*., **248**(3–4), 179–192.

De Sherbinin, A., Schiller, A. & Pulsipher, A., 2007. The vulnerability of global cities to climate hazards, *Environ. Urban.,* **19**(1), 39–64.

Fritz, H.M. & Borrero, J.C., 2006. Somalia field survey after the December 2004 Indian Ocean tsunami, *Earthq. Spectra,* **22**(S3), 219–233.

Fritz, H.M., Synolakis, C.E. & McAdoo, B.G., 2006. Maldives field survey after the December 2004 Indian Ocean tsunami, *Earthq. Spectra,* **22**(S3), 137–154.

Fujii, Y. & Satake, K., 2007. Tsunami source of the 2004 Sumatra–Andaman earthquake inferred from tide gauge and satellite data, *Bull. seism. Soc. Am.,* **97**(1A), S192–S207.

Hébert, H. & Schindelé, F., 2015. Tsunami impact computed from offshore modeling and coastal amplification laws: Insights from the 2004 Indian Ocean Tsunami, *Pure appl. Geophys.,* **172**(12), 3385–3407.

Heidarzadeh, M., Pirooz, M.D., Zaker, N.H., Yalciner, A.C., Mokhtari, M. & Esmaeily, A., 2008. Historical tsunami in the Makran subduction zone off the southern coasts of Iran and Pakistan and results of numerical modeling, *Ocean Eng*., **35**(8–9), 774–786.

Heidarzadeh, M., Pirooz, M.D., Zaker, N.H. & Yalciner, A.C., 2009. Modeling the near-field effects of the worst possible tsunami in the Makran subduction zone, *Ocean Eng*., **36**(5), 368–376.

Heidarzadeh, M., Krastel, S. & Yalciner, A.C., 2014. The state-of-the-art numerical tools for modeling landslide tsunamis: a short review, In: *Submarine Mass Movements and Their Consequences,*Krastel *et al.*(Ed.), Chap. 43, pp. 483–495, ISBN: 978-3-319-00971-1, Springer International publishing.

Heidarzadeh, M. & Satake, K., 2015. New insights into the source of the Makran tsunami of 27 November 1945 from tsunami waveforms and coastal deformation data, *Pure appl. Geophys.,* **172**(3), 621–640.

Heidarzadeh, M., Teeuw, R., Day, S. & Solana, C., 2018a. Storm wave runups and sea level variations for the September 2017 Hurricane Maria along the coast of Dominica, eastern Caribbean Sea: Evidence from field surveys and sea level data analysis, *Coast. Eng. J.,* **60**(3), 371–384.

Heidarzadeh, M., Satake, K., Takagawa, T., Rabinovich, A. & Kusumoto, S., 2018b. A comparative study of far-field tsunami amplitudes and ocean-wide propagation properties: Insight from major trans-Pacific tsunamis of 2010–2015, *Geophys. J. Int.,* **215,** 22–36.

Heidarzadeh, M., Ishibe, T., Sandanbata, O., Muhari, A. & Wijanarto, A.B., 2020. Numerical modeling of the subaerial landslide source of the 22 December 2018 Anak Krakatoa volcanic tsunami, Indonesia, *Ocean Eng*., **195,** doi:10.1016/j.oceaneng.2019.106733.

Jankaew, K., Atwater, B.F., Sawai, Y., Choowong, M., Charoentitirat, T., Martin, M.E. & Prendergast, A., 2008. Medieval forewarning of the 2004 Indian Ocean tsunami in Thailand, *Nature,* **455**(7217), 1228.

Kanamori, H., 2006. Seismological aspects of the December 2004 great Sumatra-Andaman earthquake, *Earthq. Spectra,* **22**(S3), 1–12.

Kowalik, Z., Knight, W., Logan, T. & Whitmore, P., 2007. The tsunami of 26 December 2004: Numerical modeling and energy considerations, *Pure appl. Geophys.,* **164,** 379–393.

Lay, T. *et al.*, 2005. The Great Sumatra-Andaman earthquake of 26 December 2004, *Science,* **308,** 1127–1133.

Liu, P.L.F. *et al.*, 2005. Observations by the international tsunami survey team in Sri Lanka, *Science,* **308**(5728), 1595–1595.

Løvholt, F., Pedersen, G., Bazin, S., Kühn, D., Bredesen, R.E. & Harbitz, C., 2012. Stochastic analysis of tsunami runup due to heterogeneous coseismic slip and dispersion, *J. geophys. Res.,* **117**(C03047), doi.org/10.1029/2011JC007616.

Maheshwari, B.K., Sharma, M.L. & Narayan, J.P., 2006. Geotechnical and structural damage in Tamil Nadu, India, from the December 2004 Indian Ocean tsunami, *Earthq. Spectra,* **22,** 475–493.

Mori, N. & Takahashi, T. 2011 Tohoku Earthquake Tsunami Joint Survey Group, 2012. Nationwide post event survey and analysis of the 2011 Tohoku earthquake tsunami, *Coast. Eng. J.,* **54**(1), 1250001–1.

Muhari, A. *et al.*, 2019. The December 2018 Anak Krakatau volcano tsunami as inferred from post-tsunami field surveys and spectral analysis, *Pure appl. Geophys.,* **176,** 5219–5233.

Nagarajan, B. *et al.*, 2006. The Great Tsunami of 26 December 2004: A description based on tide-gauge data from the Indian subcontinent and surrounding areas, *Earth Planets Space,* **58**(2), 211–215.

Neetu, S., Suresh, I., Shankar, R., Nagarajan, B., Sharma, R., Shenoi, S.S.C., Unnikrishnan, A.S. & Sundar, D., 2011. Trapped waves of the 27 November 1945 Makran tsunami: observations and numerical modeling, *Nat. Hazards,* **59**(3), 1609–1618.

Okada, Y., 1985. Surface deformation due to shear and tensile faults in a half-space, *Bull. seism. Soc. Am.,* **75,** 1135–1154.

Okal, E.A., 2015. The quest for wisdom: Lessons from 17 tsunamis, 2004–2014. *Phil. Trans. R. Soc. A,* **373**(2053), 20140370, doi.org/10.1098/rsta.2014.0370.

Okal, E.A. & Synolakis, C.E., 2008. Far-field tsunami hazard from mega-thrust earthquakes in the Indian Ocean, *Geophys. J. Int.,* **172**(3), 995–1015.

Okal, E.A., Fritz, H.M., Raveloson, R., Joelson, G., Pančošková, P. & Rambolamanana, G., 2006a. Madagascar field survey after the December 2004 Indian Ocean tsunami, *Earthq. Spectra,* **22**(S3), 263–283.

Okal, E.A., Fritz, H.M., Raad, P.E., Synolakis, C., Al-Shijbi, Y. & Al-Saifi, M., 2006b. Oman field survey after the December 2004 Indian Ocean tsunami, *Earthq. Spectra,* **22**(S3), 203–218.

Omira, R. *et al.*, 2019. The September 28th, 2018, tsunami in Palu-Sulawesi, Indonesia: a post-event field survey, *Pure appl. Geophys.,* **176**(4), 1379–1395.

Pugh, D. & Woodworth, P., 2014. *Sea-Level Science: Understanding Tides, Surges, Tsunamis and Mean Sea-Level Changes*. Cambridge University Press, P. 407.

Rabinovich, A.B., Thomson, R.E. & Stephenson, F.E., 2006. The Sumatra tsunami of 26 December 2004 as observed in the North Pacific and North Atlantic oceans, *Surv. Geophys*., **27**(6), 647–677.

Rabinovich, A.B. & Thomson, R.E., 2007. The 26 December 2004 Sumatra tsunami: Analysis of tide gauge data from the World Ocean Part 1. Indian Ocean and South Africa, *Pure appl. Geophys.,* **164**(2/3), 261–308.

Rabinovich, A.B., Candella, R. & Thomson, R.E., 2011a. Energy decay of the 2004 Sumatra tsunami in the world ocean, *Pure appl. Geophys.,* **168**(11), 1919–1950.

Rabinovich, A.B., Woodworth, P.L. & Titov, V.V., 2011b. Deep-sea observations and modeling of the 2004 Sumatra tsunami in Drake Passage, *Geophys. Res. Lett.,* **38** L16604, doi.org/10.1029/2011GL048305.

Rabinovich, A.B., Thomson,, R.E. & Fine, I.V., 2013. The 2010 Chilean tsunami off the west coast of Canada and the northwest coast of the United States, *Pure appl. Geophys.,* **170,** 1529–1565.

Saito, T., Inazu, D., Miyoshi, T. & Hino, R., 2014. Dispersion and nonlinear effects in the 2011 Tohoku-Oki earthquake tsunami, *J. geophys. Res.* **119**(8), 5160–5180.

Satake, K., 2014. Advances in earthquake and tsunami sciences and disaster risk reduction since the 2004 Indian Ocean tsunami, *Geosci. Lett*., **1**(1), 15, doi.org/10.1186/s40562-014-0015-7.

Satake, K. *et al.*, 2005. Report on post tsunami survey along the Myanmar coast for the December 2004 Sumatra–Andaman earthquake, *Annu. Rep. Act. Fault Paleoearthq. Res.,* **5,** 161–188.

Satake, K., Heidarzadeh, M., Quiroz, M. & Cienfuegos, R., 2020. History and features of trans-oceanic tsunamis and implications for paleo-tsunami studies, *Earth Sci. Rev.,* doi:10.1016/j.earscirev.2020.103112.

Sheth, A., Sanyal, S., Jaiswal, A. & Gandhi, P., 2006. Effects of the December 2004 Indian Ocean tsunami on the Indian mainland, *Earthq. Spectra,* **22,** 435–473.

Sibuet, J.C. *et al.*, 2007. 26th December 2004 Great Sumatra–Andaman earthquake: Co-seismic and post-seismic motions in northern Sumatra, *Earth planet. Sci. Lett.,* **263**(1–2), 88–103.

Siripong, A., 2006. Andaman seacoast of Thailand field survey after the December 2004 Indian Ocean tsunami, *Earthq. Spectra,* **22**(S3), 187–202.

Soloviev, S.L., 1978. *Tsunamis. The Assessment and Mitigation of 1481 Earthquake Risk (Natural Hazard, 1)*(pp. 118–139). Paris: 1482 UNESCO.

Synolakis, C.E. & Okal, E.A., 2005. 1992–2002: perspective on a decade of post-tsunami surveys, In: Tsunami ed. by K. Satake, *Adv. Natur. Technol. Hazards,* **23,** pp. 1–30, Springer.

Synolakis, C.E. & Bernard, E.N., 2006. Tsunami science before and beyond Boxing Day 2004, *Phil. Trans. R. Soc. A,* **364**(1845), 2231–2265.

Tilmann, F.J., Craig, T.J., Grevemeyer, I., Suwargadi, B., Kopp, H. & Flueh, E., 2010. The updip seismic/aseismic transition of the Sumatra megathrust illuminated by aftershocks of the 2004 Aceh-Andaman and 2005 Nias events, *Geophys. J. Int.,* **181**(3), 1261–1274.

Titov, V.V., Rabinovich, A.B., Mofjeld, H., Thomson, R.E. & González, F.I., 2005. The global reach of the 26 December 2004 Sumatra tsunami, *Science,* **309,** 2045–2048.

Tomita, T., Imamura, F., Arikawa, T., Yasuda, T. & Kawata, Y., 2006. Damage caused by the 2004 Indian Ocean tsunami on the southwestern coast of Sri Lanka, *Coast. Eng. J.,* **48**(02), 99–116.

Tsuji, Y. *et al.*, 2011. Field surveys of tsunami heights from the 2011 off the Pacific Coast of Tohoku, Japan Earthquake, *Bull. Earthq. Res. Inst.,* **86,** 29–279.

Watada, S., Kusumoto, S. & Satake, K., 2014. Traveltime delay and initial phase reversal of distant tsunamis coupled with the self-gravitating elastic Earth, *J. geophys. Res.,* **119**(5), 4287–4310.

Weatherall, P. *et al.*, 2015. A new digital bathymetric model of the world's oceans, *Earth Space Sci*., **2,** 331–345.

Wessel, P. & Smith, W.H.F., 1998. New, improved version of generic mapping tools released, *EOS, Trans Am. geophys. Un.,* **79**(47), 579, doi.org/10.1029/98EO00426.

Yeh, H., Chadha, R.K., Francis, M., Katada, T., Latha, G., Peterson, C., Raghuraman, G. & Singh, J.P., 2006. Tsunami runup survey along the southeast Indian coast, *Earthq. Spectra,* **22,** 173–186.